



ELSEVIER

Contents lists available at SciVerse ScienceDirect

Comptes Rendus Chimie

www.sciencedirect.com



Full paper/Mémoire

[Cu(bpdo)₂·2H₂O]²⁺-supported SBA-15 nanocatalyst for efficient one-pot synthesis of benzoxanthenone and benzochromene derivatives

Reihaneh Malakooti^{a,*}, Zeinab Parsaei^a, Rahele Hosseinabadi^a, Hossein A. Oskooie^b,
Majid M. Heravi^b, Mina Saeedi^b, Maryam Amrollah^b, Akram Fallah^b

^a Nanochemistry Research Laboratory, Department of Chemistry, University of Birjand, Birjand, Iran

^b Department of Chemistry, School of Sciences, Alzahra University, Vanak, Tehran, Iran

ARTICLE INFO

Article history:

Received 29 December 2012

Accepted after revision 18 March 2013

Available online 3 May 2013

Keywords:

[Cu(bpdo)₂·2H₂O]²⁺/SBA-15

Benzoxanthenones

Benzochromenes

Solvent-free conditions

Nanocatalyst

ABSTRACT

A novel [Cu(bpdo)₂·2H₂O]²⁺-supported SBA-15 catalyst (bpdo = 2,2'-bipyridine,1,1'-dioxide) was prepared by the impregnation method. The catalyst was characterized by XRD, TEM, and BET nitrogen adsorption–desorption method, FT-IR, UV–vis, and chemical analysis. XRD patterns and TEM analysis of [Cu(bpdo)₂·2H₂O]²⁺/SBA-15 showed highly ordered hexagonal mesoporous silica, even after immobilization. Also, nitrogen adsorption–desorption isotherms exhibited type-IV isotherms and H1 hysteresis loops according to the IUPAC classification of mesoporous materials. This green support was tested for the synthesis of benzoxanthenone and benzochromene derivatives under solvent-free conditions, with high yield of products via a simple experimental and work-up procedure.

© 2013 Académie des sciences. Published by Elsevier Masson SAS. All rights reserved.

1. Introduction

Research on mesoporous materials has grown up due to their outstanding properties [1]. MCM-41 [2] and SBA-15 [3] are the most well-known mesoporous silicas with hexagonal pore arrays and narrow pore size distributions. SBA-15 is identified by larger pore size and sidewall, lower specific surface area and higher hydrothermal stability than MCM-41. These materials are used as catalysts [4], molecular sieves [1], enzyme immobilizations [5], drug delivery [6], etc.

The immobilization of transition metals complexes onto mesoporous silica has also been of particular interest owing to their catalytic activities as heterogeneous catalysts in chemical reactions. Some attempts have been made to immobilize copper complexes, such as CuBr/bipyridine [7], Cu(acac)₂ [8], copper ammine [9], Cu(II)

cyclam [10] and [Cu(NH₃)₃(H₂O)₃]²⁺ [11] on mesoporous silica as a catalyst.

The catalytic behavior of such immobilized silica might be improved as compared with their parent ones: Cu-[2,6-bis(benzoxazolyl)pyridine]-SBA-15 for trapping and decomposing HCN [12], [Cu(NCCH₃)₆][B{C₆H₃(*m*-CF₃)₂]₄]-SBA-15 for aldehyde olefination through an aminosilane linker [13], copper oxides in mesoporous silica for the reduction of NO [14], and recently [Cu(acac)₂]-SBA-15 for aziridination of styrene [15] are some examples for this purpose.

It is supposed that metal complexes of bpdo ligand may act as good guest molecules for mesoporous silica [16] that might originate from their gauche conformations. Also, it was shown that metal bpdo complexes are water-soluble [17], which leads us to present a green procedure for the synthesis of a highly uniformly distributed immobilized mesoporous silica.

Xanthenone derivatives have attracted considerable interest because they possess various pharmaceutical activities, such as anti-bacterial [18], anti-inflammatory [19] and anti-viral [20] activities. Also, some xanthenone

* Corresponding author.

E-mail addresses: rmalakooti@birjand.ac.ir, reihaneh.malakooti@gmail.com (R. Malakooti).

derivatives have shown agricultural bactericide activity [21] and have been used in laser technology [22].

2-amino-4*H*-chromene derivatives are important classes of oxygenated heterocycles, which have attracted much interest because of the biological activities of naturally occurring representatives [23]. Some of the reported benzopyrans possess anticoagulant, anti-spasmodic, diuretic, anti-anaphylactic, anticancer, and anti-diabetic activities [24]. 4*H*-Benzo[*b*]pyrans and their derivatives are of considerable interest because of their wide range of biological activities as listed [25]. In addition, they can be used as cognitive enhancers for the treatment of neurodegenerative diseases, including Alzheimer's disease, amyotrophic lateral sclerosis, Huntington's disease, Parkinson's disease, AIDS-associated dementia, and Down syndrome, as well as for the treatment of schizophrenia and myoclonus [26].

Herein, we report the synthesis of a novel [Cu(bpdo)₂·2H₂O]²⁺-supported SBA-15 catalyst used as an efficient catalyst for the synthesis of benzoxanthenone and benzochromene derivatives by the reaction of aromatic aldehydes, α/β-naphthol, dimedone or malononitrile, respectively, under solvent-free conditions, with high yield of products; moreover, it only requires a simple experimental and work-up procedure, without using any hazardous solvent. In this research, the [Cu(bpdo)₂·2H₂O]²⁺ complex was prepared and loaded onto SBA-15 channels. Our studies showed that it can catalyze the reaction of aromatic aldehydes **1**, β-naphthol **2** and dimedone **3** efficiently under solvent-free conditions to obtain benzoxanthenone derivatives **4**.

In another investigation, benzochromene derivatives **5**/**7** were synthesized by the reaction of aromatic aldehydes **1**, α/β-naphthol **6**/**2** and malononitrile.

2. Experimental

2.1. Materials and equipments

A Bruker D8 ADVANCE diffractometer with Ni-filtered Cu Kα radiation (1.5406 Å) was used for XRD analysis. The data were recorded with a speed of 2°/min and a step of 0.05°. The FTIR spectra in the mid-IR region were also obtained with KBr pellets using a Bruker FT-IR spectrometer (Tensor 27). TEM images were obtained with a Philips CM10 electron microscope at 100 kV. N₂ adsorption–desorption isotherms were determined at 77.35 K with a Quantachrome Autosorb-1 apparatus. Before measurements, the samples were outgassed at 150 °C for 12 h. Using the Brunauer–Emmett–Teller (BET) method and Barrett–Joyner–Halenda (BJH) analyses, the specific surface area and the pore size distributions were obtained from the desorption branch of the isotherms, respectively. A Shimadzu AA-6300 flame atomic absorption spectrometer was utilized to obtain the sample concentration. For this purpose, 0.1 g of the sample was digested in HNO₃. The solution was diluted before the measurement. The melting points were measured using a capillary tube method with a Bamstead Electrothermal 9200 apparatus, whereas ¹H NMR spectra were recorded on a Bruker AQS-AVANCE spectrometer at 500 and 125 MHz, using

TMS as an internal standard in DMSO-d₆ and CDCl₃. FT-IR spectra were recorded using KBr disks on a FT-IR Bruker Tensor 27 instrument. The elemental analysis was performed with an Elementar Analysensystem GmbH VarioEL in CHNS mode.

2.2. Synthesis of nanocatalyst

2.2.1. Synthesis of the bpdo ligand

2,2'-bipyridine 1,1'-dioxide (bpdo) was synthesized according to the procedure reported in [27].

2.2.2. Synthesis of the [Cu(bpdo)₂·2H₂O]²⁺ complex

CuCl₂·2H₂O and bpdo were dissolved in deionized water with a molar ratio of 1:2. This solution was heated at 70 °C for 2 h. The complex solution was evaporated till complex precipitation. The precipitate was filtered off, dried at room temperature and a 80% yield was obtained for the synthesis of the Cu complex [17].

2.2.3. Synthesis of MCM-41 and SBA-15

MCM-41 was synthesized according to the procedure reported in [28] using the molar compositions of 1.00 SiO₂:0.54 NaOH:0.5 CTAB:0.34 HCl:100 H₂O.

SBA-15 was synthesized according to the procedure reported in [29] using the compositions of 2 g P123, 15 g H₂O, 60 g 2 M HCL and 4.25 g TEOS.

2.2.4. Immobilization of [Cu(bpdo)₂·2H₂O]²⁺ within MCM-41 or SBA-15

First, 0.2 g of the [Cu(bpdo)₂·2H₂O]²⁺ complex was dissolved in 10 mL of deionized water. Then 1 g of MCM-41 or SBA-15, which was dried overnight under vacuum at 150 °C, was added to the solution of the [Cu(bpdo)₂·2H₂O]²⁺ complex [17]. The resultant mixture was stirred for 24 h at room temperature and then filtered. Finally, the light green precipitate was washed with deionized water and dried at room temperature.

2.3. General procedure for the synthesis of benzoxanthenone derivatives

A mixture of an aromatic aldehyde (1 mmol), β-naphthol (1 mmol), dimedone (1 mmol) and [Cu(bpdo)₂·2H₂O]²⁺/SBA-15 (0.03 g) was stirred at 150 °C for an appropriate time (Table 2). After completion of the reaction, which was monitored by thin layer chromatography (TLC), ethanol was added to the mixture and the catalyst was filtered off. After the evaporation of the solvent, the precipitated crude product was recrystallized from ethanol to give the pure product. All the compounds were known and their physical data were compared with those of authentic compounds and found to be identical [30–32].

2.3.1. Spectral data for selected compound (4h)

M.p. 181–183 °C; ¹H NMR (CDCl₃, 500 MHz): δ 1.01 (s, 3H), 1.16 (s, 3H), 2.29 (d, *J* = 16.3 Hz, 1H), 2.36 (d, *J* = 16.3 Hz, 1H), 2.6 (s, 2H), 5.7 (s, 1H), 7.25–7.5 (m, 7H), 7.81–7.84 (m, 2H), 7.94 (d, *J* = 8.4 Hz, 1H) ppm; GC-MS: *m/z*: 433.

2.4. General procedure for the synthesis of benzochromenes derivatives

A mixture of an aromatic aldehyde (1 mmol), α -naphthol/ β -naphthol (1 mmol), malononitrile (1 mmol) and $[\text{Cu}(\text{bpdo})_2 \cdot 2\text{H}_2\text{O}]^{2+}/\text{SBA-15}$ (0.03 g) was stirred at 150°C for an appropriate time (Table 3). After the completion of the reaction, which was monitored by TLC, ethanol was added to the mixture and the catalyst was filtered off. After evaporation of the solvent, the precipitated crude product was recrystallized from ethanol to give the pure product. All the compounds were known and their physical data were compared with those of authentic compounds and found to be identical [33–35].

2.4.1. Spectral data for selected compound (5a)

M.p. $277\text{--}279^\circ\text{C}$; $^1\text{H NMR}$ ($\text{DMSO-}d_6$, 500 MHz): δ 7.96–7.90 (m, 2H), 7.85 (d, $J = 4.5$ Hz, 1H), 7.47–7.13 (m, 8H); 7.0 (s, 2H), 5.30 (s, 1H); GC–MS: m/z : 298.

2.5. Recycling of the catalyst

After the completion of the reaction, ethanol was added to the mixture and the catalyst was recycled by a simple filtration, washed with ethanol, dried at 80°C , and reused for the next reaction with only a modest loss in activity. The catalyst has been recovered and reused two times for the synthesis of **4a** and **5a**. The obtained results are summarized in Table 4.

3. Results and discussions

3.1. Characterization of the nanocatalyst

XRD patterns of SBA-15 (Fig. 1a) and MCM-41 (Fig. 1c) show three peaks corresponding to (100), (110) and (200) planes, which are adopted with typical two-dimensional

hexagonal symmetry [36,37]. Compared with MCM-41, SBA-15 peaks appear at lower angles, which are related to their larger pore size. After grafting of the cationic complex, $[\text{Cu}(\text{bpdo})_2 \cdot 2\text{H}_2\text{O}]^{2+}$, on the surfaces of SBA-15 and MCM-41 (Figs. 1b and d), hexagonal symmetry was conserved. Also, relative decreases are observed between the XRD intensities of the parent mesoporous and grafted samples, which originate from complex immobilization [38,39].

Fig. 2 shows the TEM image of the $[\text{Cu}(\text{bpdo})_2 \cdot 2\text{H}_2\text{O}]^{2+}/\text{SBA-15}$ nanocatalyst. It reveals that the parent mesoporous structure is retained after immobilization in agreement with XRD results, with approximately uniform distributed complexes inside the channels.

Nitrogen adsorption–desorption isotherms of SBA-15 and $[\text{Cu}(\text{bpdo})_2 \cdot 2\text{H}_2\text{O}]^{2+}/\text{SBA-15}$ are shown in Fig. 3. The corresponding data are also listed in Table 1. For both samples, the typical IV isotherms with H1-type hysteresis loop are presented at high relative pressure according to the IUPAC classification of mesoporous materials [40]. According to Table 1, the pore diameter decreases from 8.62 nm for SBA-15 to 6.14 nm for $[\text{Cu}(\text{bpdo})_2 \cdot 2\text{H}_2\text{O}]^{2+}/\text{SBA-15}$. In addition, compared with pure SBA-15, a decrease in BET surface area, pore volume, and an increase in wall thickness are also observed after immobilization. These results reconfirm the incorporation of the catalyst in the channels of SBA-15. Atomic absorption spectroscopy was also used to determine the concentration of Cu in immobilized SBA-15. Cu concentration was found to be 0.1023 mmol/g.

FT-IR spectra of the synthesized materials are plotted in Fig. 4. Bpdo spectrum (Fig. 4a) contains two bands near 845 cm^{-1} and two bands at 1220 and 1256 cm^{-1} , which are due to NO bending and NO stretching, respectively. Also, a band at 3250 cm^{-1} appeared, which corresponds to the C–H bipyridine oxide ring [27,41]. A back shift for NO stretching is observed in the spectrum of the

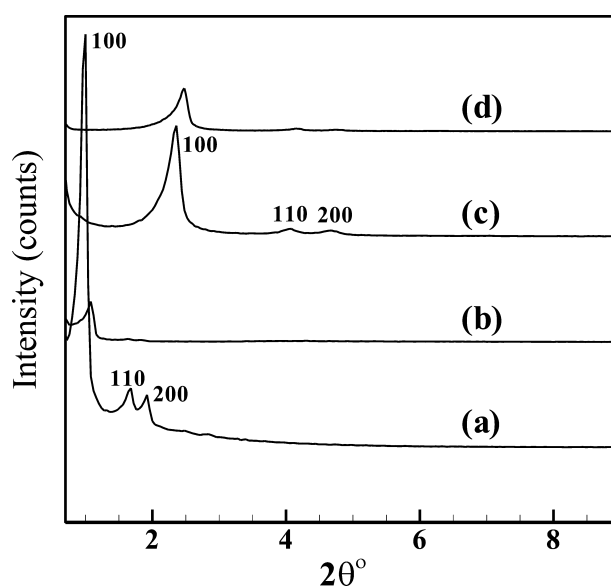


Fig. 1. X-ray diffraction patterns of SBA-15 (a), $[\text{Cu}(\text{bpdo})_2 \cdot 2\text{H}_2\text{O}]^{2+}/\text{SBA-15}$ (b), MCM-41 (c) and $[\text{Cu}(\text{bpdo})_2 \cdot 2\text{H}_2\text{O}]^{2+}/\text{MCM-41}$ (d).

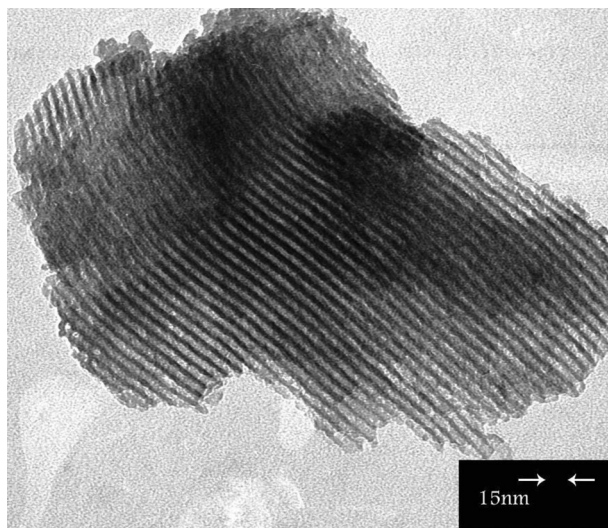


Fig. 2. Transmission electron microscopy image of the $[\text{Cu}(\text{bpdo})_2 \cdot 2\text{H}_2\text{O}]^{2+}/\text{SBA-15}$ nanocatalyst.

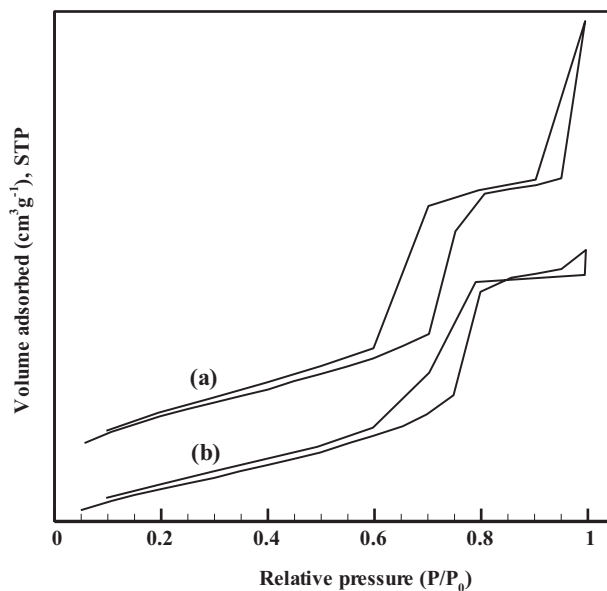


Fig. 3. Nitrogen adsorption–desorption isotherms of parent SBA-15 (a) and $[\text{Cu}(\text{bpdo})_2 \cdot 2\text{H}_2\text{O}]^{2+}/\text{SBA-15}$ (b).

$[\text{Cu}(\text{bpdo})_2 \cdot 2\text{H}_2\text{O}]^{2+}$ complex (Fig. 4b) in comparison with that of the bpdo ligand, because of its coordination [41]. MCM-41 (Fig. 4c) as well as SBA-15 (Fig. 4e) spectra are in good agreement with the literature [12,38].

The spectra of immobilized MCM-41 and SBA-15 are shown in Figs. 4d and f, respectively. The corresponding NO bending intensities decreased after immobilization. Interestingly, the pyridine ring vibrations of the complex

Table 1

Physicochemical properties of the catalysts.

Materials	$C(\text{M})$	S_{BET}	V_{BJH}	D_{BJH}^a	A_0	D_{100}	W^b
SBA-15	—	542.6	1.13	8.62	9.48	8.2	0.86
$[\text{Cu}(\text{bpdo})_2 \cdot 2\text{H}_2\text{O}]^{2+}/\text{SBA-15}$	0.1023	365.3	0.7145	6.14	10.23	8.85	4.09

$C(\text{M})$, initial concentration of metal species (mmol/g); S_{BET} , specific surface area (m^2g^{-1}); V_{BJH} , pore volume (cm^3g^{-1}); D_{BJH} , pore diameter (nm); A_0 , cell parameters (nm); D_{100} , interplanar spacing (nm); W , wall thickness (nm).

^a Calculated from the desorption branch.

^b $W = A_0 - D_{\text{BJH}}$ ($A_0 = 2 D_{100}/\sqrt{3}$).

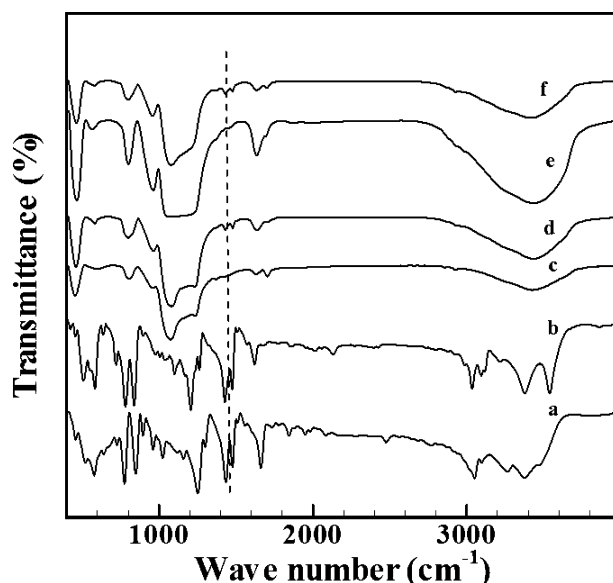


Fig. 4. FT-IR spectra of the bpdo ligand (a), $[\text{Cu}(\text{bpdo})_2 \cdot 2\text{H}_2\text{O}]^{2+}$ complex (b), MCM-41 (c), $[\text{Cu}(\text{bpdo})_2 \cdot 2\text{H}_2\text{O}]^{2+}$ -MCM-41 (d), SBA-15 (e) and $[\text{Cu}(\text{bpdo})_2 \cdot 2\text{H}_2\text{O}]^{2+}$ -SBA-15 (f).

around 1450 cm^{-1} have a similar shape in immobilized mesoporous spectra, which confirms the presence of the complex within the channels of MCM-41 [16a] and SBA-15 [42].

Fig. 5 shows the UV absorption spectra of $\text{CuCl}_2 \cdot 2\text{H}_2\text{O}$ (a), bpdo ligand (b), $[\text{Cu}(\text{bpdo})_2 \cdot 2\text{H}_2\text{O}]\text{Cl}_2$ complex (c), $[\text{Cu}(\text{bpdo})_2 \cdot 2\text{H}_2\text{O}]\text{Cl}_2/\text{SBA-15}$ (d) and SBA-15 (e) in water. The spectrum of the free bpdo ligand shows two main peaks at 217 and 260 nm, corresponding to $\pi-\pi^*$ transitions, in agreement with the literature [43]. Also, $T_{2g} \leftarrow E_{2g}$ d-d transition was observed at 800 nm for $\text{CuCl}_2 \cdot 2\text{H}_2\text{O}$ and with a slight shift around 790 nm for the $[\text{Cu}(\text{bpdo})_2 \cdot 2\text{H}_2\text{O}]\text{Cl}_2$ complex and for $[\text{Cu}(\text{bpdo})_2 \cdot 2\text{H}_2\text{O}]\text{Cl}_2/\text{SBA-15}$. It also

confirms the immobilization of the complex inside the channels of SBA-15[44].

The immobilization of $[\text{Cu}(\text{bpdo})_2 \cdot 2\text{H}_2\text{O}]^{2+}$ within MCM-41 or SBA-15 is shown in Scheme 1.

3.2. Catalytic investigations of $[\text{Cu}(\text{bpdo})_2 \cdot 2\text{H}_2\text{O}]^{2+}/\text{SBA-15}$

Herein, we have developed an environmentally friendly, simple and efficient method for the synthesis of various benzoxanthene and benzochromenes derivatives (Schemes 2 and 3). Our attempt was aimed at avoiding the use of organic solvents and of a toxic catalyst, but instead at implementing a simplistic procedure and

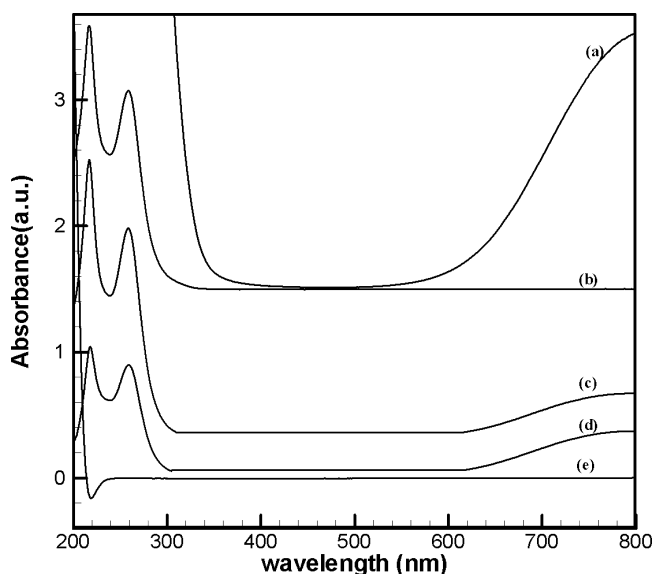
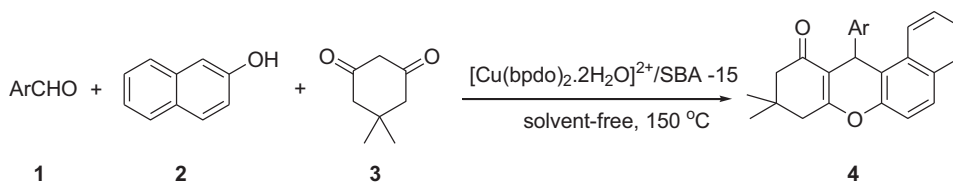
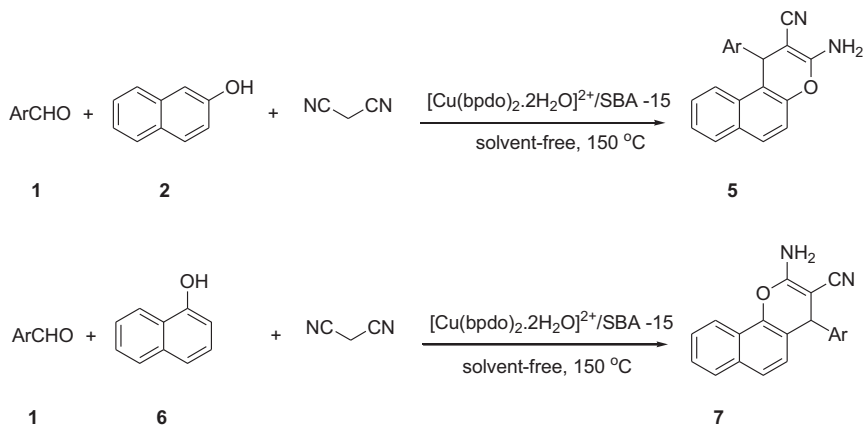


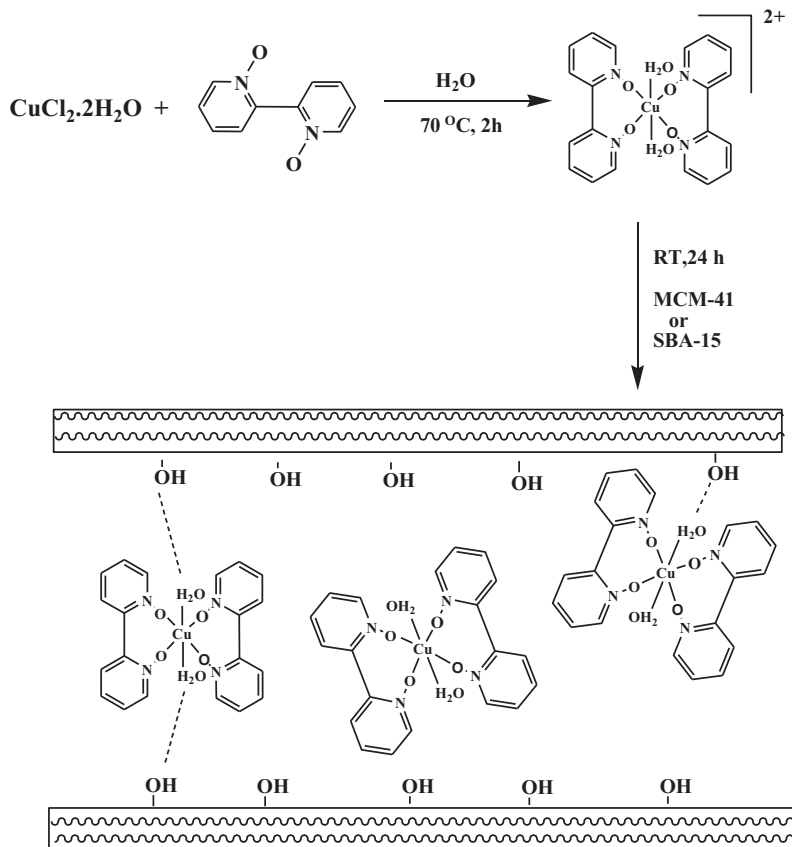
Fig. 5. UV spectra of $\text{CuCl}_2 \cdot 2\text{H}_2\text{O}$ (a), bpdo ligand (b), $[\text{Cu}(\text{bpdo})_2 \cdot 2\text{H}_2\text{O}]^{2+}$ complex (c), $[\text{Cu}(\text{bpdo})_2 \cdot 2\text{H}_2\text{O}]^{2+}$ SBA-15 (d), and SBA-15 (e).



Scheme 1. Synthesis of benzoxanthenone derivatives **4** by the reaction of aromatic aldehydes **1**, β -naphthol **2** and dimedone **3** under solvent-free conditions.



Scheme 2. Synthesis of benzochromene derivatives **5/7** by the reaction of aromatic aldehydes **1**, α -naphthol/ β -naphthol **6/2** and malononitrile under solvent-free conditions.



Scheme 3. Immobilization of the $[\text{Cu}(\text{bpdo})_2 \cdot 2\text{H}_2\text{O}]^{2+}$ complex onto SBA-15 channels.

practical reaction of aromatic aldehydes, α/β -naphthol and dimedone or malononitrile.

To choose the best reaction conditions, at first a model reaction was selected, using 1 mmol of benzaldehyde, 1 mmol of β -naphthol and 1 mmol of dimedone in the presence of 0.03 g of various catalysts, such as $[\text{Cu}(\text{bpdo})_2 \cdot 2\text{H}_2\text{O}]^{2+}/\text{MCM-41}$ (%Cu = 0.1 mmol/g) and $[\text{Cu}(\text{bpdo})_2 \cdot 2\text{H}_2\text{O}]^{2+}/\text{SBA-15}$ (%Cu = 0.11 mmol/g) under solvent-free conditions at 150 °C. The resultant product (**4a**) was obtained in high yield: (85%) for $[\text{Cu}(\text{bpdo})_2 \cdot 2\text{H}_2\text{O}]^{2+}/\text{SBA-15}$, and 70% for $[\text{Cu}(\text{bpdo})_2 \cdot 2\text{H}_2\text{O}]^{2+}/\text{MCM-41}$, after 55 min. Therefore, the best catalyst for this reaction was $[\text{Cu}(\text{bpdo})_2 \cdot 2\text{H}_2\text{O}]^{2+}/\text{SBA-15}$.

Other derivatives and resulting data are listed in Table 2. It is worthwhile to mention that no by-products were observed. The model reaction was achieved in the absence of catalyst and, in this conditions, with poor yields (5%). In addition, different amounts of the catalyst were investigated, and it was found that the best results were obtained in the presence of 0.03 g of $[\text{Cu}(\text{bpdo})_2 \cdot 2\text{H}_2\text{O}]^{2+}/\text{SBA-15}$; with a larger amount of catalyst, no significant difference in yield was observed. In another examination, the model reaction was carried out in different solvents, such as dichloromethane and ethanol. In these cases, the corresponding product was obtained in very poor yields.

In another experiment, the reaction of 1 mmol of benzaldehyde, 1 mmol of β -naphthol and 1 mmol of malononitrile was carried out in the presence of catalytic amounts of $[\text{Cu}(\text{bpdo})_2 \cdot 2\text{H}_2\text{O}]^{2+}/\text{SBA-15}$, under solvent-free conditions.

It was found that in the presence of 0.03 g of catalyst, at 150 °C, the corresponding product was obtained in very good yields. Under these conditions, a series of benzochromene (benzoxanthrone) derivatives were synthesized by the reaction of different aromatic aldehydes, α/β -naphthol and malononitrile (dimedone). In addition, the model reaction was examined for different amounts of the catalyst; it was found that the best results were obtained in the presence of 0.03 g of $[\text{Cu}(\text{bpdo})_2 \cdot 2\text{H}_2\text{O}]^{2+}/\text{SBA-15}$. Also, the model reaction was carried out in different solvents; the best reaction conditions proved to be attained in the absence of solvent.

It is noteworthy to mention that the effect of the nature of the substituent on the aromatic ring showed no obvious effect on these reactions, because they were obtained in high yields in relatively short reaction times, as shown in Tables 2 and 3.

After the completion of the reaction, the catalyst was recycled by simple filtration, washed, dried, and reused for the next reaction with only a modest loss in activity. The

Table 2
Synthesis of benzoxanthrone derivatives **4** by the reaction of aromatic aldehydes **1**, β -naphthol **2** and dimedone **3** under solvent-free conditions.

Entry	Ar	Time (min)	Product	Yield (%) ^a	mp (°C)	
					Found	Reported
1	C ₆ H ₅	55	4a	85	152–153	151–153 [27]
2	4-OHC ₆ H ₄	70	4b	85	224–227	223–225 [27]
3	4-MeC ₆ H ₄	60	4c	90	178–179	176–178 [27]
4	4-NO ₂ C ₆ H ₄	45	4c	88	178–179	178–180 [28]
5	4-MeOC ₆ H ₄	60	4e	90	205–207	204–205 [27]
6	4-ClC ₆ H ₄	50	4f	95	183–184	180–182 [28]
7	3-NO ₂ C ₆ H ₄	60	4g	85	169–171	168–170 [28]
8	4-BrC ₆ H ₄	50	4h	90	181–183	186–187 [29]
9	4-FC ₆ H ₄	50	4i	93	187–188	185–186 [29]

^a Yields refer to the isolated products.

Table 3
Synthesis of benzochromenes derivatives **5/7** by the reaction of aromatic aldehydes **1**, α -naphthol/ β -naphthol **6/2** and malononitrile under solvent-free conditions.

Entry	Ar	Time (min)	Product	Yield (%) ^a	mp (°C)	
					Found	Reported
1	C ₆ H ₅	15	5a	90	277–279	278–279 [30]
2	4-ClC ₆ H ₄	10	5b	85	219–221	217–220 [31]
3	4-NO ₂ C ₆ H ₄	20	5c	95	184–185	185–186 [30]
4	4-BrC ₆ H ₄	15	5d	85	220–223	221–222 [30]
5	3-NO ₂ C ₆ H ₄	20	5e	85	239–240	239–241 [31]
6	4-FC ₆ H ₄	20	5f	80	238–240	237–238 [30]
7	4-MeOC ₆ H ₄	10	5g	75	181–182	182–183 [32]
8	4-MeC ₆ H ₄	15	5h	80	252–254	253–254 [30]
9	4-BrC ₆ H ₄	15	7a	75	240–242	241–243 [31]
10	C ₆ H ₅	15	7b	85	212–215	215–217 [31]
11	4-ClC ₆ H ₄	10	7c	85	246–248	245–248 [31]
12	4-NO ₂ C ₆ H ₄	10	7d	90	241–243	240 [32]
13	3-NO ₂ C ₆ H ₄	15	7e	85	211–213	212 [32]

^a Yields refer to isolated products.

Table 4
Reusability of the catalyst in the synthesis of **4a** and **5a**.

Entry	Number of recycle	Yield (%) ^a of 4a	Yield (%) ^a of 5a
1	Fresh	85	90
2	1	85	90
3	2	80	85

^a Yields refer to isolated products.

catalyst has been recovered and reused two times for the synthesis of **4a** and **5a**. The obtained results are summarized in Table 4.

4. Conclusion

In conclusion, a new heterogeneous catalyst based on cationic copper (II) complex-supported SBA-15 is proposed; its efficiency was investigated in the synthesis of benzoxanthenone and benzochromene derivatives. This procedure offers several advantages, including cleaner reaction and high product yields, as well as a simple experimental and work-up procedure, which makes it a useful and attractive process for the synthesis of these compounds. Moreover, no hazardous solvent has been used for these reactions.

Acknowledgment

The authors are thankful to University of Birjand and Alzahra University for financial support of this study.

References

- [1] A. Corma, *Chem. Rev.* 97 (1997) 2373.
- [2] C.-Y. Chen, H.-X. Li, M.E. Davis, *Microporous Mater.* 2 (1993) 17.
- [3] M. Kruk, M. Jaroniec, C.H. Ko, R. Ryoo, *Chem. Mater.* 12 (2000) 1961.
- [4] A. Taguchi, F. Schüth, *Microporous Mesoporous Mater.* 77 (2005) 1.
- [5] J. Lee, J. Kim, J. Kim, H. Jia, M.I. Kim, J.H. Kwak, S. Jin, A. Dohnalkova, H.G. Park, H.N. Chang, P. Wang, J.W. Grate, T. Hyeon, *Small* 1 (2005) 744.
- [6] M. Vallet-Regí, F. Balas, D. Arcos, *Angew. Chem. Int. Ed.* 46 (2007) 7548.
- [7] J.V. Nguyen, C.W. Jones, *Macromolecules* 37 (2004) 1190.
- [8] P. Kustrowski, L. Chmielarz, R. Dziembaj, P. Cool, E.F. Vansant, *J. Phys. Chem. B* 109 (2005) 11552.
- [9] L. Jiao, J.R. Regalbutto, *J. Catal.* 260 (2008) 342.
- [10] S. Goubert-Renaudin, M. Etienne, S. Brandes, M. Meyer, F. Denat, B. Lebeau, A. Walcarius, *Langmuir* 25 (2009) 9804.
- [11] N. Brodie-Linder, R. Besse, F. Audonnet, S. LeCaer, J. Deschamps, M. Impéror-Clerc, C. Alba-Simionesco, *Microporous Mesoporous Mater.* 132 (2010) 518.
- [12] M.J. Hudson, J.P. Knowles, P.J.F. Harris, D.B. Jackson, M.J. Chinn, J.L. Ward, *Microporous Mesoporous Mater.* 75 (2004) 121.
- [13] A. Sakthivel, A.K. Hijazi, A.I. Al Hmaideen, F.E. Kuhn, *Microporous Mesoporous Mater.* 96 (2006) 293.
- [14] L. Chmielarz, P. Kuśtrowski, R. Dziembaj, P. Cool, E.F. Vansant, *Appl. Catal. B, Environ.* 62 (2006) 369.
- [15] C. Pereira, K. Biernacki, S.L.H. Rebelo, A.L. Magalhesa, A.P. Carvalho, J. Pires, C. Freire, *J. Mol. Catal. A: Chem.* 312 (2009) 53.
- [16] (a) R. Malakooti, F. Farzaneh, M. Ghandi, *J. Sci., Islam. Repub. Iran* 17 (2006) 43 ;
(b) M.M. Heravi, H.A. Oskooie, R. Malakooti, B. Alimadadi, H. Alinejad, F.K. Behbahani, *Catal. Commun.* 10 (2009) 819.
- [17] G.L. Zheng, Y.Y. Li, S.Y. Song, H.J. Zhang, *Chem. Commun* (2008) 4918.
- [18] T. Hideu [Jpn. Tokkyo Koho JP 56005480,1981).
- [19] H.N. Hafez, M.I. Hegab, I.S. Ahmed-Farag, A.B.A. El-Gazzar, *Bioorg. Med. Chem. Lett.* 18 (2008) 4538.
- [20] J.P. Poupelin, G. Saint-Ruf, O. Foussard-Blanpin, G. Narcisse, G. Uchida-Ernouf, R. Lacroix, *Eur. J. Med. Chem.* 13 (1978) 67.
- [21] J. Li, W. Tang, L. Lu, W. Su, *Tetrahedron Lett.* 49 (2008) 7117.
- [22] S. M. Menchen, S.C. Benson, J.Y. L. Lam, W. Zhen, D. Sun, B.B. Rosenblum, S.H. Khan, M. Taing (US Patent 6583168, 2003).
- [23] (a) J.D. Hepworth, C.D.B.M. Gabbutt, in : A.R. Katritzky, C.W. Ress, E.F.V. Scriven (Eds.), *Comprehensive Heterocyclic Chemistry II*, Pergamon Press, Oxford, 1995, pp. 301–468 ;
(b) C.R. Green, J.M. Evans, A.K. Vong, in : A.R. Katritzky, C.W. Ress, E.F.V. Scriven (Eds.), *Comprehensive Heterocyclic Chemistry II*, Pergamon Press, Oxford, 1995, p. 470 ;
(c) W.F. Hoffman, A.W. Alberts, P.S. Anderson, J.S. Chen, R.L. Smith, A.K. Willard, *J. Med. Chem.* 29 (1986) 849.
- [24] (a) H. Koga, H. Sato, T. Ishizawa, H. Nabata, (US Patent 5614633, 1997) ;
(b) H. Kuenzer, R.F. Jautelat, L. Zorn, C. H. Hartung, (US Patent 6844336B2, 2005).
- [25] L. Bonsignore, G. Loy, D. Secci, A.A. Calignano, *Eur. J. Med. Chem.* 28 (1993) 517.
- [26] C. S. Konkoy, D.B. Fick, S.X. Cai, N.C. Lan, J. F. W. Keana (Patent 0075123, 2000 Chem. Abstr. 2001, 134, 29313a).
- [27] P.G. Simpson, A. Vinciguerra, J.V. Quagliano, *Inorg. Chem.* 2 (1963) 282.
- [28] Q.-H. Xia, K. Hidajat, S. Kawi, *Mater. Lett.* 42 (2000) 102.
- [29] (a) D. Zhao, J. Feng, Q. Huo, N. Melosh, G.H. Fredrickson, B.F. Chmelka, G.D. Stucky, *Science* 279 (1998) 548 ;
(b) D. Zhao, Q. Huo, J. Feng, B.F. Chmelka, G.D. Stucky, *J. Am. Chem. Soc.* 120 (1998) 6024.
- [30] W.H. Zhang, X.B. Lu, J.H. Xiu, Z.L. Hua, L.X. Zhang, M.G.C. Nandi, S. Samai, R. Kumar, M.S. Singh, *Tetrahedron* 65 (2009) 7129.
- [31] J. Li, J. Fang, W. Su, *Synth. Commun.* 40 (2010) 1029.
- [32] Z.-H. Zhang, P. Zhang, S.-H. Yang, H.-J. Wang, J. Deng, *J. Chem. Sci.* 122 (2010) 427.
- [33] X.-S. Wang, G.-S. Yang, G. Zhao, *Tetrahedron: Asymmetry* 19 (2008) 709.
- [34] S. Balalaie, S. Ramezanpour, M. Bararjanian, J.H. Gross, *Synth. Commun.* 38 (2008) 1078.
- [35] M.M. Heravi, K. Bakhtiari, V. Zadsirjan, F.F. Bamoharram, O.M. Heravi, *Bioorg. Med. Chem. Lett.* 17 (2007) 4262.
- [36] N.K.K. Raj, S.S. Deshpande, R.H. Ingle, T. Raja, P. Manikandan, *Catal. Lett.* 98 (2004) 217.
- [37] C.-H. Lee, H.-C. Lin, S.-H. Cheng, T.-S. Lin, C.-Y. Mou, *J. Phys. Chem. C* 113 (2009) 16058.
- [38] A. Sakthivel, A.K. Hijazi, M. Hanzlik, A.S.T. Chiang, F.E. Kuhn, *Appl. Catal. A* 294 (2005) 162.
- [39] C.T. Kresge, M.E. Leonowicz, W.J. Roth, J.C. Vartuli, J.S. Beck, *Nature* 359 (1992) 710.
- [40] W.-H. Zhang, X.-B. Lu, J.-H. Xiu, Z.-L. Hua, L.-X. Zhang, M. Robertson, J.-L. Shi, D.S. Yan, J.D. Holmes, *Adv. Funct. Mater.* 14 (2004) 544.
- [41] A. Vinciguerra, P.G. Simpson, Y. Kakiuti, J.V. Quagliano, *Inorg. Chem.* 2 (1963) 286.
- [42] H.G. Manyar, E. Gianotti, Y. Sakamoto, O. Terasaki, S. Coluccia, S. Tumbiolo, *J. Phys. Chem. C* 112 (2008) 18110.
- [43] H. Kanno, J. Yamamoto, S. Murahashi, S. Utsuno, J. Fujita, *Bull. Chem. Soc. Jpn.* 64 (1991) 2936.
- [44] S.K. Madan, W.E. Bull, *J. Inorg. Nucl. Chem.* 26 (1964) 2211.